The Journal of Eukaryotic Microbiology

ISOP Published by the International Society of Protistologists

Journal of Eukaryotic Microbiology ISSN 1066-5234

ORIGINAL ARTICLE

A Widely Distributed Thraustochytrid Parasite of Diatoms Isolated from the Arctic Represents a gen. and sp. nov.

Brandon T. Hassett

UiT Norges arktiske universtiet, BFE, NFH bygget, Framstredet 6, 9019, Tromsø, Norway

Keywords
Labyrinthulea; Labyrinthulomycetes; Thraustochytriidae.

Correspondence
B.T. Hassett, UiT Norges arktiske universtiet, BFE, NFH bygget, Framstredet 6, 9019 Tromsø, Norway
Telephone number: +4777645711; FAX number: +19077824461; e-mail: brandon.hassett@uit.no

Received: 18 September 2019; revised 23 March 2020; accepted March 25, 2020.
Early View publication April 29, 2020

doi:10.1111/jeu.12796

ABSTRACT

A unicellular, heterotrophic, eukaryotic parasite was isolated from nearshore Arctic marine sediment in association with the diatom *Pleurosigma* sp. The parasite possessed ectoplasmic threads that could penetrate diatom frustules. Healthy and reproducing *Pleurosigma* cultures would begin to collapse within a week following the introduction of this parasite. The parasite (2–10 μm diameter) could reproduce epibiotically with biflagellate zoospores, as well as binary division inside and outside the diatom host. While the parasite grew, diatom intracellular content disappeared. Evaluation of electron micrographs from co-cultures revealed the presence of hollow tubular processes and amorphic cells that could transcend the diatom frustule, generally at the girdle band, as well as typical thraustochytrid ultrastructure, such as the presence of bothrosomes. After nucleotide extraction, amplification, and cloning, database queries of DNA revealed closest molecular affinity to environmental thraustochytrid clone sequences. Testing of phylogenetic hypotheses consistently grouped this unknown parasite within the *Thraustochytriidae* on a distinct branch within the environmental sequence clade Lab19. Reclassification of Arctic high-throughput sequencing data, with appended reference datasets that included this diatom parasite, indicated that the majority of thraustochytrid sequences, previously binned as unclassifiable stramenopiles, are allied to this new isolate. Based on the combined information acquired from electron microscopy, life history, and phylogenetic testing, this unknown isolate is described as a novel species and genus.

THE *Labyrinthulea* are heterotrophic eukaryotic stramenopiles historically considered morphologically distinct by the presence of an ectoplasmic net (Tsui et al. 2009) that is used to interface nutrient acquisition and motility (Bennett et al. 2017).The *Labyrinthulea* are generally divided into three morphologically distinct groups, based on the utility and function of the ectoplasmic net: the labyrinthulids, thraustochytrids, and the aplanochytrids (Leander et al. 2004). The most recent molecular phylogenies suggest that *Labyrinthulea* is comprised of at least four orders: *Amphitremida*, *Labyrinthulida*, *Oblongichytrida*, and *Thraustochytrida* (Pan et al. 2017), with the possibility of several additional orders that remain phylogenetically unresolved (Bennett et al. 2017). Within *Thraustochytrida,* there are at least two families: the *Thraustochytriidae* and *Althorniidae* (containing one genus, *Althornia*). *Thraustochytriidae* is the most diverse taxonomic family within the *Thraustochytrida* that circumscribes numerous genera: *Aurantiochytrium*, *Botryochytrium*, *Hondaea*, *Labyrinthulochytrium*, *Monorhizochytrium*, *Parietichytrium*, *Schizochytrium*, *Sicyoidochytrium*, *Thraustochytrium*, and *Ulkenia* (Bahnweg and Sparrow 1974; Dellero et al. 2018; Doi and Honda 2017; Hassett and Gradinger 2018; Yokoyama and Honda 2007; Yokoyama et al. 2007), with additional genera not yet represented in sequence databases (Pan et al. 2017).

Labyrinthulea have been cultured and detected by molecular methods throughout the global marine realm (Bai et al. 2019; Bochdansky et al. 2017; Pan et al. 2017). Ecologically, *Labyrinthulea* behave as bacteriovores, saprotrophs, and symbionts in marine ecosystems (Bennett et al. 2017) and are implicated as important degraders of coastal detritus (Raghukumar 2002; Ueda et al. 2015) and marine snow (Bochdansky et al. 2017). Members of

Labyrinthulea can associate with photosynthetic organisms as substrate for development (Scholz et al. 2016). However, parasitism of photosynthetic organisms by this group is atypically reported. Consequently, the ecological role of *Labyrinthulea* as algal parasites is nebulous. Ambiguity surrounding the parasitic nature of *Labyrinthulea* is heightened by observations of these organisms at the tips of filamentous algae (Raghukumar 2006) and on senescent and moribund diatoms (Raghukumar 1986), suggesting these organisms are opportunists, as opposed to pathogens that have co-evolved to parasitize. Select *Labyrinthulea* members within the aplanochytrids and *Labyrinthula* can consume (Popova et al. 2020) and parasitize diatoms with their ectoplasmic nets (Hamamoto and Honda 2019); however, few observations (Gaertner 1979) have ever reported thraustochytrids parasitizing healthy diatom cells. As a result, the relevance of *Labyrinthulea* algal parasites to marine ecosystems remains unknown.

A coculture of a pennate diatom within the genus *Pleurosigma* was established with an unknown parasite that was isolated from Arctic marine sediment in Tromsø, Norway. Analysis of this parasite revealed closest molecular affinity to environmental clone sequences generated in New York, USA, and the recently described Norwegian isolate, *Labyrinthulochytrium arktikum*. Microscopic examination of this isolate revealed a unique life history, primarily the ability to parasitize diatoms by penetrating their frustules with ectoplasmic threads. Phylogenetic analyses using deoxyribonucleic acid (DNA)-encoding regions of the 18S small ribosomal subunit (18S rRNA) locus place this unknown isolate among the diverse thraustochytrids in the family *Thraustochytriida*. Based on phylogenetic testing, contextualized with reference trees (Pan et al. 2017), ultrastructure, and life history, this unknown isolate is described as a new genus, *Phycophthorum* (gen. nov.) and species *Phycophthorum isakeiti* (sp. nov.).

MATERIALS AND METHODS

Isolation and culture

A surface sediment sample was collected from the nearshore marine environment outside of Tromsø, Norway (N69.632 E18.906), on January 21, 2019, at the end of the polar night. Sediment was aliquoted into Petri dishes and diluted with unfiltered natural seawater. Diluted sediment was explored for the presence of parasitized *Pleurosigma* sp. diatoms with an inverted microscope (Leica DM IL, Wetzlar, Germany). Diatoms identified as *Pleurosigma* sp. that were hosting parasites were harvested from sediment with a pipette, re-suspended in sterile seawater, and incubated in 96-well plates with a *Pleurosigma* sp. isolated in Helgoland, Germany (Buaya et al. 2019). After stable cocultures were established, initially free of other foreign or contaminating species, isolates were maintained at 12 °C with a light:dark cycle of 14 h:10 h in f/2 medium. The temperature and light–dark cycle used in this study was adopted from the original conditions used to cultivate and maintain the diatom in Helgoland, Germany. Cocultures were transferred to PmTG (peptonized milk, tryptone, and glucose) agar media, as well as f/2 nutrient media, and explored for the presence of diatom-independent growth. In addition, a supplemental growth analysis was conducted using various media (Daniel Powers, unpublished thesis): GPY, Honda, KMV, and MC (Rosa et al. 2011).

DNA extraction, amplification, and sequencing

Biomass from liquid cocultures was concentrated on 0.2 μm filters (Sartorious, Göttingen, Germany). Genomic DNA was extracted from filters using the DNeasy PowerSoil Kit (Qiagen, Hilden, Germany) and subsequently amplified using polymerase chain reaction (PCR) with Platinum Taq (Thermo Fisher Scientific, Waltham, MA) and the 18S rRNA primer sets NS1/NS4 (5′-GTAGTCATATGCTTGTCTC-3′/5′-CTTCCGTCAATTCCTTTAAG-3′) and NS5/NS8 (5′-AACTTAAAGGAATTGACGGAAG-3′/5′-TCCGCAGGTTCACCTACGGA-3′) (White et al. 1990). Amplicons were purified with the PureLink Quick PCR Purification Kit (Thermo Fisher Scientific). Purified amplicons were gel-eluted and blunt-end cloned into the EcoRV restriction site of pUC57-Kan. Sanger sequencing was conducted using the M13R and M13F primers on a 3730xl DNA Analyzer (Applied Biosystems, Foster City, CA). Sequencing was conducted bidirectionally to maximize confidence in base calls along the length of the amplicon. Chromatographs were examined with MEGA v7.0.26 (Kumar et al. 2016) to assess the accuracy of automated base calls and to explore the presence of single nucleotide polymorphisms (SNPs). The final sequence (NCBI accession MN382127) was used for phylogenetic analysis.

Microscopy

Transmission electron microscopy

Cocultures were grown in fresh f/2 media for 2 wk and fixed at 4 °C with 0.075% ruthenium red, 4% formaldehyde, and 2.5% glutaraldehyde in f/2 for 2 h. This fixation cocktail was then exchanged for 4% formaldehyde and 2.5% glutaraldehyde in PHEM buffer (PIPES, HEPES, EGTA, magnesium sulphate heptahydrate) and left overnight at 4 °C. The samples were rinsed with PHEM, postfixed with 1% OsO_4 in ddH_2O for 2 h, rinsed again, and dehydrated in a graded series of ethanol (30%, 60%, 90%, 96%, and 100%), before a final embedding in epoxy resin (EPON). Sections were contrasted with uranyl acetate and lead citrate. Imaging was conducted with a JEM-1010 electron microscope (JEOL, Tokyo, Japan).

Scanning electron microscopy

Samples were fixed with 4% formaldehyde and 2.5% glutaraldehyde in PHEM-buffered f/2. Samples were then rinsed three times with PHEM buffer and subsequently postfixed with 1% OsO_4 in ddH_2O for 1 h. After postfixing, samples were rinsed three times with PHEM buffer and then dehydrated in a graded series of ethanol (30%, 60%, 90%, and 96% for 15 min and then in absolute

ethanol three times for 15 min). Samples were dried using an EM CPD300 (Leica). The samples were then mounted on scanning electron microscopy stubs with quick-drying silver paint and coated with gold/palladium in a Polaron Sputter Coater (Quorum Technologies, Lewes, UK). Imaging was conducted with a Zeiss Sigma (Jena, Germany) with an in-lens detector at 2kV.

Phylogenetic analysis

Basic Local Alignment Search Tool (BLAST) queries were conducted with clone sequences against the National Center for Biotechnology Information (NCBI)'s nucleotide database and subsequently sorted as diatom or thraustochytrid. Sequences allied to the thraustochytrids were parsed, oriented, and aligned. Multiple sequence alignments (MSAs) were created de novo from sequences (minimum 1,200 base pairs length) retrieved from the NCBI nucleotide database. These sequences were aligned in MEGA7 using MUSCLE (−400 gap penalty). Unalignable regions were eliminated from the MSA. The MSA was then end-trimmed. Bayesian posterior probabilities were generated in MrBayes v3.2.7a (Ronquist et al. 2012) using the GTR + I + G model with 10,000,000 generations, with sampling events occurring once every 100 generations and a "burnin" value of 2,500,000 generations, as previously described (FioRito et al. 2016). The consensus tree from this analysis and corresponding alignment were imported into MEGA7 and analyzed with Maximum Likelihood methods with 1,000 pseudoreplications.

The alignment previously used to generate reference trees (Pan et al. 2017) was imported into MEGA7. The assembled DNA clone sequence from the diatom parasite was appended to this MSA and manually aligned (File S1 and Table S1). This MSA was analyzed with RAxML using the rapid hill climbing algorithm and GTRCATI evolutionary model, as previously described (Pan et al. 2017) with the T-Rex web server (Boc et al. 2012). Trees were then imported into FigTree (v1.4.4) for formatting and presentation (Rambaut et al. 2018).

High-throughput sequencing

High-throughput sequencing (HTS) databases that target the 18S V3-V4 and V9 loci previously generated throughout the Arctic Ocean (NCBI BioSample accessions SAMN08888918-948, SAMN03769253-264, SAMN04555549-62) were re-processed with a manually appended SILVA (v123) database. Specifically, the parasite clone sequence and *Labyrinthulochytrium arktikum* (NCBI AccessionMG099001) were aligned against the SILVA (v123) database with default parameters in Mothur (v1.40.5, Schloss et al. 2009). This aligned sequence was then added to the existing SILVA (v123) database (Unix "cat" command). Environmental HTS reads were then reclassified with this expanded reference database using the "classify.seqs" command (Kozich et al. 2013) with default parameters.

RESULTS

Taxonomy

Phycophthorum B.T. Hassett, gen. nov.

ZooBank:urn:lsid:zoobank.org:pub:8C2DBAF2-B7EF-4B67-AE84-C2605E6ACCB8

Late disposita. Epibiotica et endobioticaque quae divisione binaria reproducunt. Motilia sunt hyalinaque. Aetates vegetativae epibioticae cellularum endobioticarum plerumque sphaeroes (II–X micrometrorum diametri). Parasiti diatomis actionum cavarum. Cellulae bothrosomia, vacuolia, complexus lipidos, et mitochonria cristis cavis continent. Aliis generis cernenda secundum collectionem molecularem, parasitismum diatomarum actionum cavarum.

Widely distributed. Epibiotic and endobiotic reproduction by binary division. Motile and hyaline. Epibiotic and endobiotic vegetative cells usually spheroidal (2–10 μm in diameter). Parasitizes diatoms with tubular processes. Cells contain bothrosomes, vacuoles, lipid inclusions, and mitochondria with tubular cristae. Distinguished from other genera based on molecular inference, parasitism of diatoms with tubular process.

Gender*:* Masculine

Etymology: Phyco = algae, Phtheirein = to destroy

Type species: *Phycophthorum isakeiti* B.T. Hassett

Phycophthorum isakeiti B.T. Hassett, sp. nov.

ZooBank: urn:lsid:zoobank.org:act:E4526C74-9FD2-4B30-A3BE-1898806851FE

Late disposita. Symbiotica diatomo marina Pleurosigmate. Zoospora, sporangia,et cellulavegetativa hyalina. Cellularumepibioticarumet endobioticarum. Reproductio endobiotica divisione binaria. Cellulae endobioticae vegetativae sphaeroes (II–X micrometrorum diametri) atque infrequenter indigestae. Reproductio epibiotica divisione binaria. Sporangium epibioticum habent zoospororum. Zoospora motila biflagellata aliquantum forma ellipsis (II micrometrorum diametri) atque subfusiformae aspectu laterali oblongaque microscopia electrorum perscrutantium. Zoospora fila longa habent quae migrationem.Cellulae motilia residet atque frustulum actionis cavae penetrat. Cellula bothrosomia, mitochondria cristis cavis, vacuolia, et complexus lipidos continet. Murus cellulae lamellarum concretus quae actionem cavam coniunctam creare possunt.

Widely distributed. Symbiotic with the marine diatom *Pleurosigma*. Zoospores, sporangia, and vegetative cells hyaline. Cells epibiotic and endobiotic. Epibiotic and endobiotic reproduction by binary division. Vegetative cells spheroidal (2–10 μm diameter) and infrequently amorphic. Motile biflagellate zoospores slightly oval (2 μm diameter) and appear subfusiform in lateral view and oblong with scanning electron microscopy. Motile cell settles and penetrates frustule with tubular process. Cell contains bothrosomes, mitochondria with tubular cristae, vacuoles, and lipid inclusions. Cell wall comprised of lamellae that can form a contiguous tubular process.

Type material*:* The name-bearing type (hapanotype) is Smithsonian Institute, catalog number: USNM1613222;

consisting of cells fixed and embedded in a transmission electron microscopy block.
Type host: *Pleurosigma* sp. diatoms
Etymology: Named in honor of the plant pathologist Dr. Thomas Isakeit.
Holotype locality: Tromsø, Norway (N69.632 E18.906)
Habitat: From nearshore marine sediment. Molecularly from northern Atlantic water, Arctic Ocean sea ice, and Arctic Ocean seawater
NCBI Accession: MN382127

Microscopy analysis

Light microscopic analysis of environmental sediment samples revealed the presence of numerous spherical hyaline cells in association with *Pleurosigma* sp. diatoms that had a noticeable loss of chlorophyll content. After successive rounds of sub-culturing, cocultures of *Pleurosigma* cells from Helgoland and this unknown parasite were established. Repeated co-culturing revealed that viable cultures of chlorophyll-rich diatoms would be decimated with the introduction of this parasite. Three days after the parasite was introduced into diatom cultures, biflagellate zoospores (2 μm in diameter) migrated and clustered around diatoms. Zoospores then interacted with the outer surface of the diatom frustule with ectoplasmic threads (Video S1, Fig. 1A) that frequently exceeded 80 μm in length. After several hours, the zoospore appeared to contact the diatom cell surface (Fig. 1B). After five days, maturing hyaline cells appeared on the outside and inside of the diatom frustule (Fig. 1C). Endobiotic cells were capable of forming larger amorphoric cells (Fig. 1D). Endobiotic *P. isakeiti* cells possessed ectoplasmic threads that facilitated slow movement and were capable of reproducing by binary division, eventually resulting in numerous cells dispersed throughout the inside of diatom frustules (Fig. 1D, E).Repeated rounds of binary division of *P. isakeiti* resulted in diatom cells bursting, releasing *Phycophthorum* cells, and leaving a broken exterior flap of frustule nearly perpendicular to the diatom (Fig. 1F). Epibiotic *Phycophthorum* cells were observed reproducing by binary division. Further differentiation resulted in the formation of a sporangium with subsequent zoospore (8–20) release (Fig. 1G). Some immature epibiotic cells began forming an amorphic appendage that could transcend the diatom frustule through a narrow break (Fig. 1H). Cellular content of parasitized diatoms first turned brown and then retracted toward the center (Fig. 1D) and in some instances toward the tips of the diatom, ultimately leading to the demise of diatom cells (Fig. 1I). Presumed *Phycophthorum* cells (~1 μm diameter) were frequently observed rapidly swarming and darting among moribund diatoms. However, the relevance of these cells to the infection process was unsuccessfully determined with light microscopy. Repeated attempts to grow the isolate on various media were unsuccessful.

Scanning electron microscopy revealed biflagellate zoospores 2 μm in diameter. One of these flagella possessed mastigonemes (Fig. 2A) that were able to interact with the diatom frustule (Fig. 2B). Many ectoplasmic threads exceeded 80 μm (Fig. 2C). Mature epibiotic cells were observed in various stages of binary division (Fig. 2D), some appearing fused with dorsally protruding daughter cells (~1 μm diameter). Epibiotic cells were observed producing ectoplasmic threads that could penetrate the diatom frustule at the girdle band (Fig. 2E). Ectoplasmic threads frequently emanated from the top of thraustochytrid cells (Fig. 2E). Epibiotic cells formed large aggregates that were intermixed with extruded diatom content (Fig. 2F).

Transmission electron microscopy revealed cells comprised of multilayered lamellar cell walls. Cell walls could form a contiguous electron-dense ectoplasmic thread that bridged dividing (Fig. 3A) and recently divided cells (Fig. 3B). This ectoplasmic thread connected cell walls to the interior of other cells (Fig. 3A). Cells contained a single Golgi body in association with a single nucleus (Fig. 3B, C), lipid inclusions (Fig. 3B), and vacuoles (Fig. 3B). Bothrosomes were visible at the base of ectoplasmic threads (Fig. 3D). Mitochondria possessed tubular cristae (Fig. 3E). Zoospores possessed a nucleus adjacent to a mitochondrion, as well as a single vacuole and lipid inclusions (Fig. 3F). Cells were frequently observed, many with vesicles protruding from the cell membrane (Fig. 3G, H). Closer examination of *Pleurosigma* diatoms revealed endogenous thraustochytrid cells (Fig. 3I), as well as ectoplasmic threads crossing the diatom frustule (Fig. 3J). Many thraustochytrid cells were observed in close association with the outside of diatom frustules, frequently with membrane interfacing cells (Fig. 3K). Ectoplasmic threads were observed inside the diatom (Fig. 3L).

Molecular analysis

After successful transformation, 10 clones for each primer set were Sanger sequenced. Analysis of BLAST results identified that all clone sequences generated with the NS1–NS4 primer set were allied to thraustochytrids. When all NS1–NS4 clones were aligned, oriented, and trimmed, there were three high-quality (i.e. well-defined chromatogram peaks) SNPs observed. Analysis of BLAST results identified that eight clone sequences generated with the NS5-NS8 primer set were allied to diatoms and two clones (one sequenced 5′–3′ orientation and the second sequenced 3′–5′orientation) to thraustochytrids. When the thraustochytrid-allied NS5–NS8 sequences were aligned and oriented, there were no SNPs observed. BLAST queries of the isolate's 18S gene revealed closest molecular affinity to a clone sequence (NCBI accession FJ800589) generated in Long Island, New York, USA (98%, 77% query coverage). The most molecularly similar described species allied to this unknown isolate was *Labyrinthulochytrium arktikum* (also isolated in Tromsø, Norway, Hassett and Gradinger 2018) with 90% identity and 100% query coverage.

To uniformly test evolutionary hypotheses within the *Labyrinthulea*, phylogenetic trees were inferred with Maximum Likelihood methods generated with the GTR

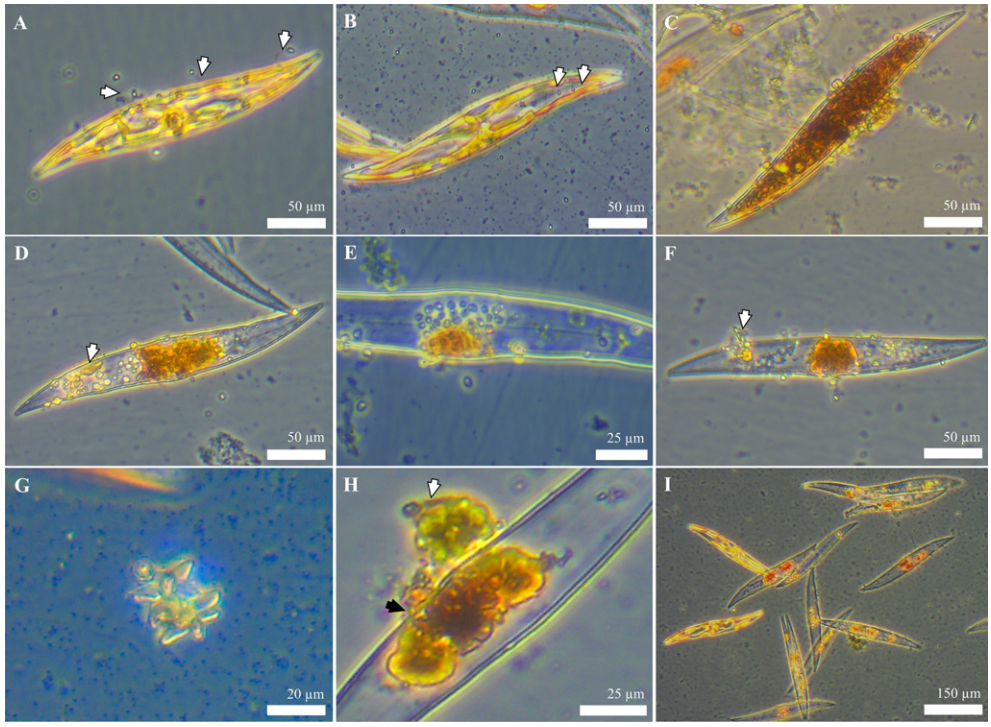

Figure 1 Light microscopy using phase contrast of *Phycophthorum isakeiti*. (**A**) Several zoospores possessing ectoplasmic threads (white arrows) used to interact with the surface of a healthy diatom cell. (**B**) Settled zoospores (white arrows) on surface of diatom frustule. (**C**) Numerous epibiotic and endobiotic thraustochytrid cells associated with the diatom. (**D**) Parasitized diatom cell with endobiotic and epibiotic cells, some forming larger amorphic cells (white arrow). (**E**) Epibiotic and endobiotic thraustochytrid cells associating with a diatom, whose intracellular contents have nearly disappeared. (**F**) Moribund diatom with flap of ruptured frustule (white arrow) hosting numerous thraustochytrid cells. (**G**) Sporangium separated from diatom frustule containing > 8 cells. (**H**) Epibiotic sporangium (white arrow) with appendage transcending diatom frustule (black arrow). (**I**) Representative overview of diatom-*P. isakeiti* coculture showing healthy and diseased cells in variable stages of infection.

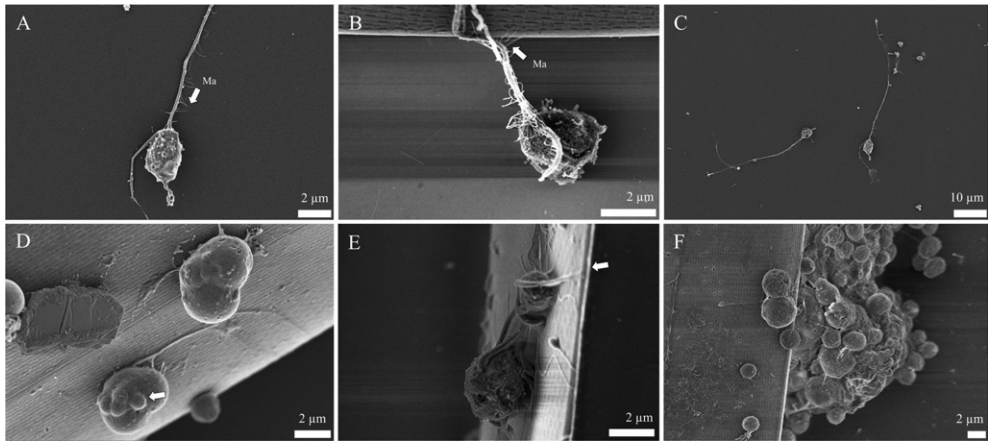

Figure 2 Scanning electron micrographs of *Phycophthorum isakeiti*. (**A**) Maturing biflagellate zoospore with mastigonemes (arrow). (**B**) Zoospore with mastigonemes interacting with diatom frustule (arrow). (**C**) Overview of maturing biflagellate zoospore with long ectoplasmic thread. (**D**) Mature epibiotic cells possessing ectoplasmic threads and reproducing by binary division. Small daughter cells appear to be emerging from one of these mature cells (white arrow). (**E**) Epibiotic cells with dorsally emanating ectoplasmic threads penetrating diatom girdle band (white arrow). Small, uncharacterized cell in foreground. (**F**) Ruptured diatom with protruding intracellular contents intermixed with thraustochytrid cells.

model (FioRito et al. 2016). The final MSA alignment included 1,163 positions. Maximum Likelihood inferences consistently produced tree topologies that grouped *P. isakeiti* within the *Thraustochytriidae,* allied phylogenetically to the clone sequence generated in New York, USA, supported with high posterior node probabilities (100% support). Several clades from this de novo analysis formed polytomies (Fig. 4). To

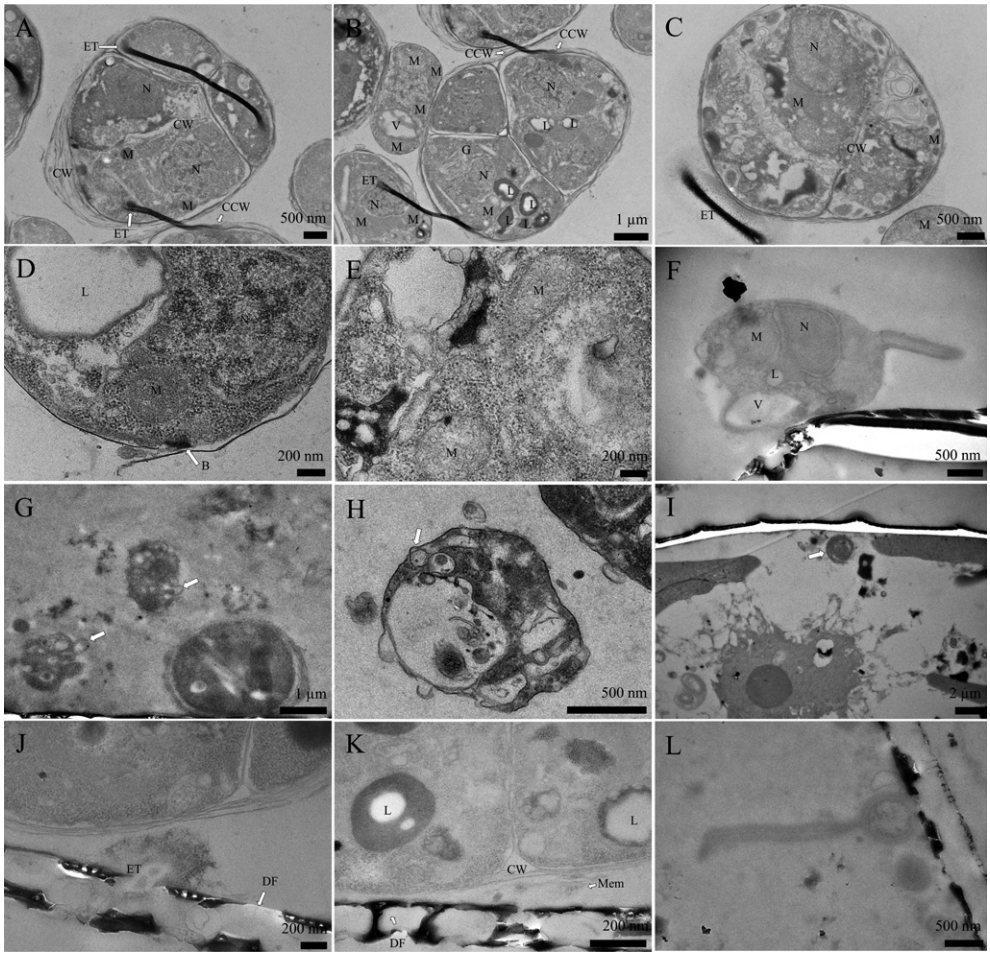

Figure 3 Abbreviations used: B = Bothrosome; CW = Cell wall; CCW = contiguous cell wall; DF = diatom frustule; ET = ectoplasmic thread; G = Golgi body; L = lipid; M = mitochondria; Mem = membrane; N = nucleus/nuclei; V = vacuoles. Transmission electron micrographs of *Phycophthorum isakeiti*. (**A**) Dividing cells with multilayered lamellar cell wall, mitochondria, nuclei, cell wall, and a hollow ectoplasmic thread, contiguous with the cell wall that connects dividing cells and recently divided cells. (**B**) Recently divided cells, connected by an electron-dense ectoplasmic thread that shares a cell wall. Cells contain a Golgi body, in association with a nucleus. Cells contain numerous lipid inclusions and vacuoles. (**C**) Overview of dividing cell and electron-dense ectoplasmic thread adjacent to cell. (**D**) *P. isakeiti* cell with partially stained lipid inclusions and bothrosome at the base of ectoplasmic thread. (**E**) Mitochondria with tubular cristae. (**F**) Zoospore in association with diatom frustule, containing a mitochondrion, nucleus, lipid inclusions, and vacuole. (**G**) Cells with protruding vesicles (white arrow). (**H**) Overview of a cell with protruding vesicle (white arrow). (**I**) Diatom cell containing a thraustochytrid (white arrow) near inside of diatom frustule. (**J**) Multilayered and hollow ectoplasmic thread penetrating diatom frustule. (**K**) *P. isakeiti* cell in association with diatom frustule with membrane interfacing cells. (**L**) Ectoplasmic thread inside diatom emanating from thraustochytrid cell.

supplement this de novo analysis, the diatom parasite was manually aligned against a prealigned database used to generate reference trees (Pan et al. 2017). In this expanded analysis, the diatom parasite grouped within *Thraustochytriidae* and formed a long branch adjacent to "Lab19" sequences (Fig. 5) that contains the New York clone, as well as a sequence from the Baltic Sea (96% support).

High-throughput sequencing

Prior to expanding the reference database with *P. isakeiti* and *Labyrinthulochytrium arktikum*, only 4,223 18S rRNA V9 sequences from the Arctic Ocean environmental sequence datasets were classified as *Labyrinthulea*. However, upon expansion of the database with *P. isakeiti* and *L. arktikum*, the total number of sequences classified as *Labyrinthulea* increased to 344,431, corresponding to a reduction in "unclassifiable stramenopiles" by 474,312 sequences. From all classified *Labyrinthulea* sequences in this appended database, 339,827 (98.6%) were allied to *P. isakeiti*. Reprocessing of V3–V4 databases with the expanded reference dataset, primarily from Utqiagvik (Barrow), Alaska, revealed that 9,449 sequences were classified as *Labyrinthulea*. Of these, 7,840 sequences were classified as *P. isakeiti*. Sequences classified as *P. isakeiti* were detected in 20 m sediment trap samples, at depths exceeding 200 m, in sea ice, and in surface seawater.

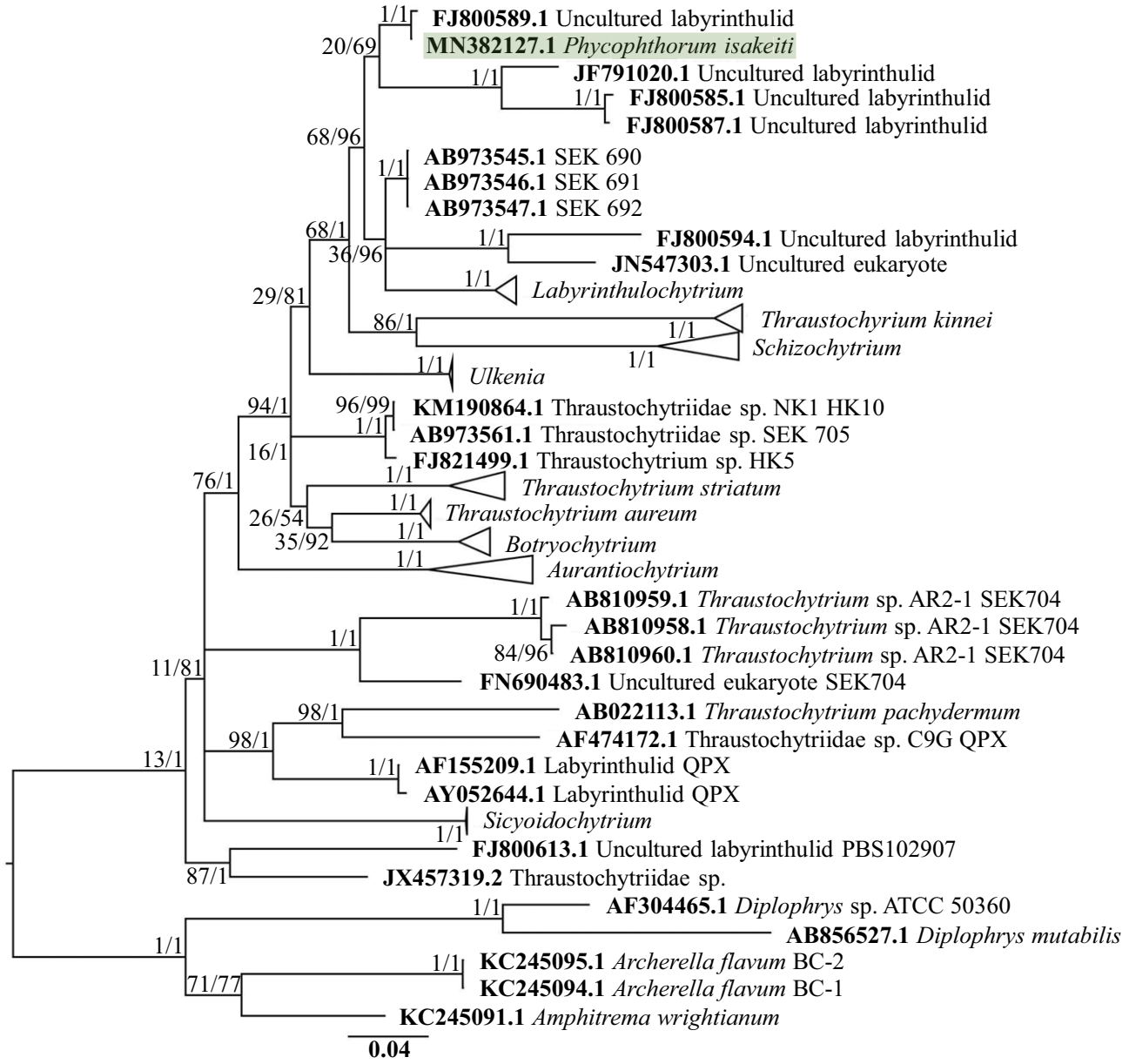

Figure 4 De novo consensus tree generated with MrBayes of 18S rRNA gene data. N with node values depict Maximum Likelihood (ML) and Bayesian posterior probabilities (ML/BPP). *Phycophthorum isakeiti* is highlighted near the top of the tree. Probabilities of 100 have been abbreviated to 1.

DISCUSSION

In this study, a thraustochytrid with atypical life history and morphology was isolated from the Arctic marine realm. Thraustochytrids are more abundant in water temperatures > 5 °C (Pan et al. 2017), but have been frequently isolated from high-latitude seas (Hassett and Gradinger 2018; Moro et al. 2003; Naganuma et al. 2006). Ecologically, this isolate is currently unique among the thraustochytrids, as it parasitizes healthy diatoms. Diatom parasitism by thraustochytrids is seldom reported. Consequently, thraustochytrids are almost exclusively considered saprobes of detritus and opportunistic parasites of marine animals (Liu et al. 2009). In this study, a combination of electron microscopy, light microscopy, and repeated co-culturing observations underscore that this isolate is capable of parasitizing viable, nonmoribund diatoms by penetrating the frustule at the girdle band, resulting in the demise of diatom cells. In the environment, thraustochytrid abundances marginally regress with chlorophyll *a* (correlation coefficient = 0.06–0.32) (Kimura et al. 2001; Raghukumar et al. 2001; Ueda et al. 2015; Liu et al.

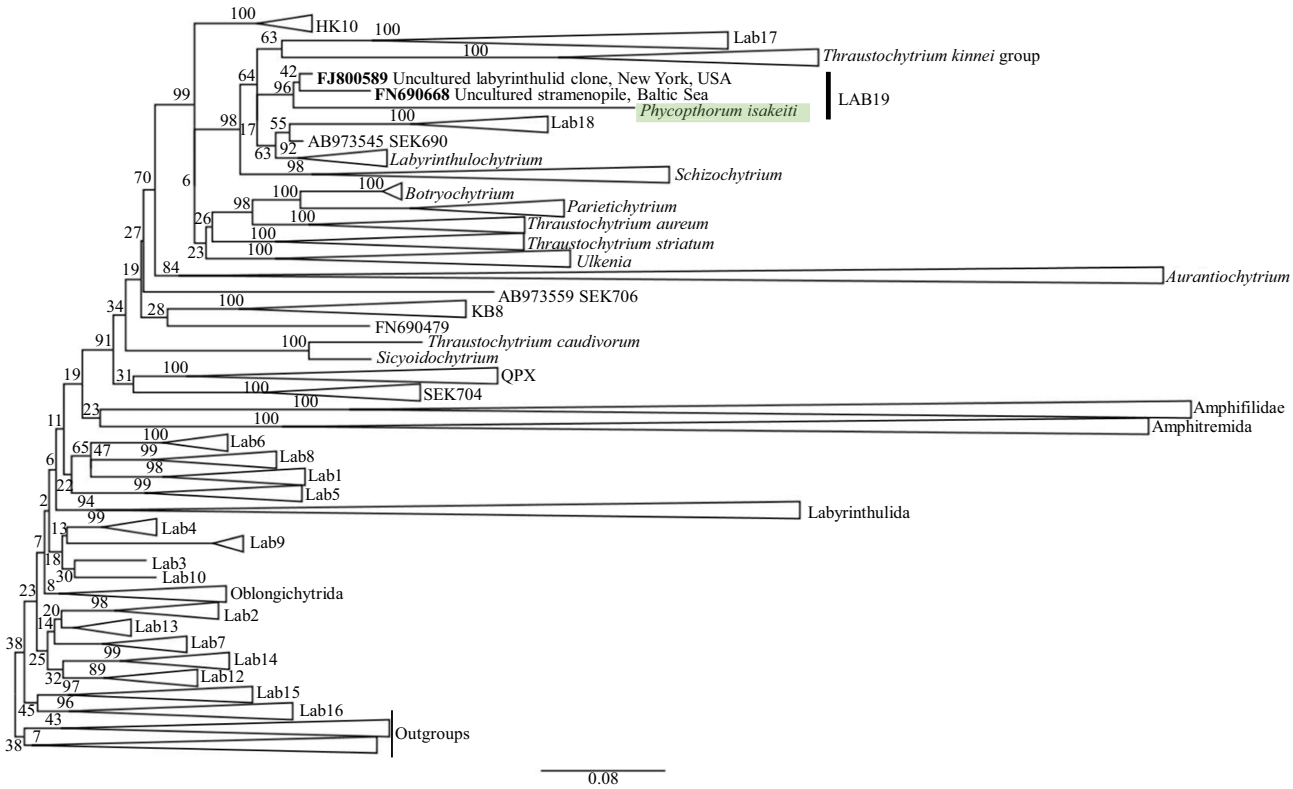

Figure 5 Pan et al. (2017) 18S rRNA reference tree expanded with *Phycophthorum isakeiti* and reprocessed in RAxML. *Phycophthorum isakeiti* forms a branch (taxon highlighted in green) sister to the Lab18-SEK690-*Labyrinthulochytrium* clade.

2017), generally ascribed to the metabolism of algae-derived organic molecules (Damare and Raghukumar 2008). Ultimately, if algal parasitism is a widely distributed phenomenon, the marginal relationship between chlorophyll *a* and thraustochytrid abundances could be partially explained by previously uncharacterized algal parasitism.

The specific ecological relevance of *P. isakeiti* and the environmental factors that regulate its population size remain to be elucidated. The detection of *P. isakeiti*-classified sequences at > 200 m depth, as well as in sediment trap material, indicates diatom-associated vertical flux, as reported elsewhere in the Arctic (Rapp et al. 2018). It is challenging to discern if its detection in the deeper ocean can be accurately ascribed to simply vertical flux or alternatively to sustained reproduction in the aphotic zone. This isolate was cocultured at the end of the polar night when primary production is arrested or marginal (Berge et al. 2015). The absence of new photosynthates to sustain saprotrophic growth under aphotic conditions might induce opportunistic or facultative parasitism. However, diatom parasitism was readily observed in the presence of artificial light, under controlled laboratory conditions. Moreover, attempts to culture this parasite in the presence of known carbon sources on conventional thraustochytrid agar media were unsuccessful. Consequently, this isolate appears to have a nutritional affinity for *Pleurosigma* sp. diatoms.

Ectoplasmic threads frequently emanated from the top of diatom-associated thraustochytrid cells. This morphological feature (i.e. dorsal as opposed to basal emanation), in addition to long migrating ectoplasmic threads, inhibited the ability to generate a micrograph of a contiguous thraustochytrid structure entering the diatom from an epibiotic thraustochytrid cell. The general mechanism of frustule penetration with an ectoplasmic thread is conserved between related *Labyrinthulea* algal parasites (Hamamoto and Honda 2019), suggesting that other *Labyrinthulea* lineages might be diatom parasites. TEM cross sections of *P. isakeiti* revealed numerous membrane-bound vesicles. The type and utility of these membrane-bound vesicles is unknown. However, it is possible that these vesicles contain degradative enzymes used to facilitate the osmotrophic life style of *Labyrinthulea* (Bongiorni et al. 2005; Taoka et al. 2009). The small cells observed with various types of microscopy, in addition to mature epibiotic cells appearing fused (Fig. 2D), suggest a possible sexual cycle, as previously reported (Ganuza et al. 2019). If true, these small cells could help explain why *Labyrinthulea*-allied sequences have been recovered and reported from among the picoplankton (de Vargas et al. 2015).

The phylogenetic position of *P. isakeiti* is within "Lab19," which contains one sequence from New York and one from the Baltic Sea. Within this larger clade, *P.*

isakeiti forms a well-supported, moderately long branch. Longer, divergent phylogenetic branches are not uncommon for organisms under positive selection arising from pathogen–host arms races (Abbott 2014; Bromham et al. 2013). The moderate length of *P. isakeiti*'s branch length suggests a degree of positive selection or alternatively, divergence due to sexual recombination. Tests of phylogenetic hypotheses using formally described taxa produced tree topologies with well-supported terminal clades, several forming a polytomy. These poytomies were generally resolved by expanding the total number of sequences used in the analysis with reference tree sequences that are more representative of actual *Labyrinthulea* diversity. The placement of *P. isakeiti* among several environmental sequence clades underscores that this isolate represents novel recovered diversity. Future characterizations of cultured isolates and molecular phylogenies expanded with additional environmental sequence data will elucidate evolutionary relationships among *Phycophthorum*, *Labyrinthulochytrium*, and their nearest branching relatives.

Differential colony morphology on agar media and lipid composition is used to distinguish and discern select *Labyrinthulea* clades (Dellero et al. 2018; FioRito et al. 2016). However, morphological observations that require agar media are difficult to ascertain for putative biotrophs and other fastidious organisms, thereby necessitating supplemental methodologies to assess diversity and robustly interpret evolutionary patterns. As thraustochytrid diversity continues to be described, molecular phylogenies based on nucleotide information will guide inferences of evolution among the *Labyrinthulea* (Damare and Raghukumar 2006; Yokoyama et al. 2007). If diatom parasitism is conserved among members of *Phycophthorum*, media-based culturing efforts (Rosa et al. 2011) would likely not capture diversity within this new genus, possibly explaining why members in this group, and potentially other environmental sequence clades, have evaded cultivation, to-date.

Reprocessing of 18S rRNA high-throughput sequencing databases identified that the majority of *Labyrinthulea* detected in the HTS eukaryotic microbial survey were allied to *P. isakeiti*. Sequences allied to *P. isakeiti* were detected throughout the Arctic Ocean in various environments (sediment, sea ice, open ocean), underscoring the potential wide distribution of this new isolate, while supporting broad dispersal suppositions that were informed by close molecular affinity to a New York clone. The approximate doubling of *Labyrinthulea*-classified HTS reads, while concurrently approximately halving "unclassifiable stramenopiles," with the addition of two reference sequences suggests that thraustochytrids are underrepresented in HTS-based surveys. Consequently, the relevance of this group to larger ecological process, such as biogeochemical cycling, and the regulation of algal bloom dynamics are likely underreported and consequently underappreciated.

Ultimately, this new isolate expands the known ecology and biodiversity of the thraustochytrids. The life history, sequence identity, and phylogenetic placement among numerous undescribed clades suggest this isolate represents a gen. et sp. nov.

ACKNOWLEDGMENTS

This research has been jointly funded by UiT the Arctic university of Norway and the Tromsø Research Foundation under the project "Arctic Seasonal Ice Zone Ecology," project number 01vm/h15. I would like to acknowledge Marti A. Arumi for his technical laboratory support and his efforts to maintain cocultures. I would also like to acknowledge Augusta Aspar and Randi Olsen at UiT for their assistance with electron microscopy.

LITERATURE CITED

Abbott, C. L. 2014. Evolution: hidden at the end of a very long branch. *Curr. Biol.*, 24:R271–R273.

Bahnweg, G. & Sparrow, F. K. 1974. Four new species of *Thraustochytrium* from Antarctic regions, with notes on the distribution of zoosporic fungi in the Antarctic marine ecosystems. *Am. J. Bot.*, 61:754–766.

Bai, M., Sen, B., Wang, Q., Xie, Y., He, Y. & Wang, G. 2019. Molecular detection and spatiotemporal characterization of Labyrinthulomycete protist diversity in the coastal waters along the Pearl River Delta. *Microb. Ecol.*, 77:394–405.

Bennett, R. M., Honda, D., Beakes, G. W. & Thines, M. 2017. Labryinthulomycota. *In:* Archibald, J. M., Simpson, A. G. B. & Slamovits, C. H. (ed.), The Handbook of the Protists, 2nd ed. Springer International Publishing, Gewerbestrasse. 14:507–542.

Berge, J., Renaud, P. E., Darnis, G., Cottier, F., Last, K., Gabrielsen, T. M., Johnsen, G., Seuthe, L., Weslawski, J. M., Leu, E., Moline, M., Nahrgang, J., Søreide, J. E., Varpe, Ø., Lønne, O. J., Daase, M. & Falk-Petersen, S. 2015. In the dark: a review of ecosystem processes during the Arctic polar night. *Prog. Oceanogr.*, 139:258–271.

Boc, A., Diallo, A. B. & Makarenkov, V. 2012. T-REX: a web server for inferring, validating and visualizing phylogenetic trees and networks. *Nucleic Acids Res.*, 40:W573–W579.

Bochdansky, A. B., Clouse, M. A. & Herndl, G. J. 2017. Eukaryotic microbes, principally fungi and labyrinthulomycetes, dominate biomass on bathypelagic marine snow. *ISME J.*, 11:362–373.

Bongiorni, L., Pusceddu, A. & Danovaro, R. 2005. Enzymatic activities of epiphytic and benthic thraustochytrids involved in organic matter degradation. *Aquat. Microb. Ecol.*, 41:299–305.

Bromham, L., Cowman, P. F. & Lanfear, R. 2013. Parasitic plants have increased rates of molecular evolution across all three genomes. *BMC Evol. Biol.*, 13:126.

Buaya, A., Kraberg, A. & Thines, M. 2019. Dual culture of the oomycete *Lagenisma coscinodisci* Drebes and *Coscinodiscus* diatoms as a model for plankton/parasite interactions. *Helgol. Mar. Res.*, 73:2.

Damare, V. & Raghukumar, S. 2006. Morphology and physiology of the marine straminipilan fungi, the aplanochytrids isolated from the equatorial Indian Ocean. *Indian J. Mar. Sci.*, 35:326–340.

Damare, V. & Raghukumar, S. 2008. Abundance of thraustochytrids and bacteria in the equatorial Indian Ocean, in relation to transparent exopolymeric particles (TEPs). *FEMS Microbiol. Ecol.*, 65:40–49.

de Vargas, C., Audic, S., Henry, N., Decelle, J., Mahé, F., Logares, R., Lara, E., Berney, C., Le Bescot, N., Probert, I., Carmichael, M., Poulain, J., Romac, S., Colin, S., Aury, J.M., Bittner, L.,

Chaffron, S., Dunthorn, M., Engelen, S., Flegontova, O., Guidi, L., Horák, A., Jaillon, O., Lima-Mendez, G., Lukeš, J., Malviya, S., Morard, R., Mulot, M., Scalco, E., Siano, R., Vincent, F., Zingone, A., Dimier, C., Picheral, M., Searson, S., Kandels-Lewis, S., Acinas, A. G., Bork, P., Bowler, C., Gorsky, G., Grimsley, N., Hingamp, P., Iudicone, D., Not, F., Ogata, H., Pesant, S., Raes, J., Sieracki, M. E., Speich, S., Stemmann, L., Sunagawa, S., Weissenbach, J., Wincker, P. & Karsenti, E. 2015. Eukaryotic plankton diversity in the sunlit ocean. *Science*, 348:1261605.

Dellero, Y., Cagnac, O., Rose, S., Seddiki, K., Cussac, M., Morabito, C., Lupette, J., Cigliano, R. A., Sanseverino, W., Kuntz, M., Jouhet, J., Maréchal, E., Rébeillé, F. & Armato, A. 2018. Proposal of a new thraustochytrid genus *Hondaea* gen. nov. and comparison of its lipid dynamics with the closely related pseudo-cryptic genus *Aurantiochytrium*. *Algal Res.*, 35:125–141.

Doi, K. & Honda, D. 2017. Proposal of *Monorhizochytrium globosum* gen. nov., com. nov. (Stramenopiles, Labyrinthulomycetes) for former *Thraustochytrium globosum* based on morphological features and phylogenetic relationships. *Phycol. Res.*, 65:188–201.

FioRito, R., Leander, C. & Leander, B. 2016. Characterization of three novel species of Labyrinthulomycota isolated from ochre sea stars (*Pisaster ochraceus*). *Mar. Biol.*, 163:170.

Gaertner, A. 1979. Some fungal parasites found in the diatom populations of the Rosfjord area (south Norway) during March 1979. *Veroff. Inst. Meeresforsch. Bremerh.*, 18:29–33.

Ganuza, E., Yang, S., Amezquita, M., Giraldo-Silva, A. & Andersen, R. A. 2019. Genomics, biology, and phylogeny *Aurantiochytrium acetophilum* sp. nov. (Thraustochytriaceae), including first evidence of sexual reproduction. *Protist*, 170:209–232.

Hamamoto, Y. & Honda, D. 2019. Nutritional intake of *Aplanochytrium* (Labyrinthulea, Stramenopiles) from living diatoms revealed by culture experiments suggesting the new prey-predator interactions in the grazing food web of the marine ecosystem. *PLoS ONE*, 14:c0208941.

Hassett, B. T. & Gradinger, R. 2018. New species of saprobic Labyrinthulea (=Labyrinthulomycota) and the erection of a gen. nov. to resolve molecular polyphyly within the aplanochytrids. *J. Eukaryot. Microbiol.*, 65:475–483.

Kimura, H., Sato, M., Sugiyama, C. & Naganuma, T. 2001. Coupling of thraustochytrids and POM, and of bacterio- and phytoplankton in a semi-enclosed coastal area: implication for different substrate preference by the planktonic decomposers. *Aquat. Microb. Ecol.*, 25:293–300.

Kozich, J. J., Westcott, S. L., Baxter, N. T., Highlander, S. K. & Schloss, P. D. 2013. Development of a dual-index sequencing strategy and curation pipeline for analyzing amplicon sequence data on the MiSeq Illumina sequencing platform. *Appl. Environ. Microbiol.*, 79:5112–5120.

Kumar, S., Stecher, G. & Tamura, K. 2016. MEGA7: molecular evolutionary genetics analysis version 7.0. for bigger datasets. *Mol. Biol. Evol.*, 33:1870–1874.

Leander, C. A., Porter, D. & Leander, B. S. 2004. Comparative morphology and molecular phylogeny of aplanochytrids (Labyrinthulomycota). *Eur. J. Protistol.*, 40:317–328.

Liu, Q., Allam, B. & Collier, J. L. 2009. Quantitative real-time PCR assay for QPX (Thraustochytriidae), a parasite of the hard clam (*Mercenaria mercenaria*). *Appl. Environ. Microbiol.*, 75:4913–4918.

Liu, Y., Singh, P., Liang, Y. Li, J., Xie, N., Song, Z., Daroch, M., Leng, K., Johnson, Z. I. & Wang, G., 2017. Abundance and molecular diversity of thraustochytrids in coastal waters of southern China. *FEMS Microbiol. Ecol.*, 93:fix070.

Moro, I., Negrisolo, E., Callegaro, A. & Andreoli, C. 2003. *Aplanochytrium stocchinoi*: a new Labyrinthulomycota from the Southern Ocean (Ross Sea, Antarctica). *Protist*, 154:331–340.

Naganuma, T., Kimura, H., Karimoto, R. & Pimenov, N. V. 2006. Abundance of planktonic thraustochytrids and bacteria and the concentration of particulate ATP in the Greenland and Norwegian Seas. *Polar Biosci.*, 20:37–45.

Pan, J., Del Campo, J. & Keeling, P. J. 2017. Reference tree and environmental sequence diversity of Labyrinthulomycetes. *J. Eukaryot. Microbiol.*, 64:88–96.

Popova, O. V., Belevich, T. A., Golyshev, S. A., Kireev, I. I. & Aleoshin, V. V. 2020. *Labyrinthula diatomea* n. sp. – a labyrinthulid associated with marine diatoms. *J. Eukaryot. Microbiol.*, https://doi.org/10.1111/jeu.12789

Raghukumar, C. 1986. Thraustochytrid fungi associated with marine algae. *Indian J. Mar. Sci.*, 15:121–122.

Raghukumar, S. 2002. Ecology of the marine protists, the Labyrinthulomycetes (Thraustochytrids and Labyrinthulids). *Eur. J. Protistol.*, 38:127–145.

Raghukumar, C. 2006. Algal-fungal interactions in the marine ecosystem: Symbiosis to parasitism. *In:* Tewari, I. (ed.), Recent Advances on Applied Aspects of Indian Marine Algae With Reference to Global Scenario. Volume 1. Central Salt and Marine Chemicals Research Institute. p. 366–385.

Raghukumar, S., Ramaiah, N. & Raghukumar, C. 2001. Dynamics of thraustochytrid protists in the water column of the Arabian Sea. *Aquat. Microb. Ecol.*, 24:175–186.

Rambaut, A., Suchard, M. A., Xie, D. & Drummond, A. J. 2018. FigTree v1.4.4. Available at: https://github.com/rambaut/figtree/releases. Accessed 1 September 2019.

Rapp, J. Z., Fernández-Méndez, M., Bienhold, C. & Boetius, A. 2018. Effects of ice-algal aggregate export on the connectivity of bacterial communities in the Central Arctic Ocean. *Front. Microbiol.*, 9:1035.

Ronquist, F., Teslenko, M., van der Mark, P., Ayres, D. L., Darling, A., Höhna, S., Larget, B., Liu, L., Suchard, M. A. & Huelsenbeck, J. P. 2012. MrBayes 3.2: efficient Bayesian phylogenetic inference and model choice across a large model space. *Syst. Biol.*, 61:539–542.

Rosa, S. M., Galvagno, M. A. & Vélez, C. G. 2011. Adjusting culture conditions to isolate thraustochytrids from temperate and cold environments in southern Argentina. *Mycoscience*, 52:242–252.

Schloss, P. D., Westcott, S. L., Ryabin, T., Hall, J. R., Hartmann, M., Hollister, E. B., Lesniewski, R. A., Oakley, B. B., Parks, D. H., Robinson, C. J., Sahl, J. W., Stres, B., Thallinger, G. G., Van Horn, D. J. & Weber, C. F. 2009. Introducing mothur: open-source, platform-independent, community-supported software for describing and comparing microbial communities. *Appl. Environ. Microbiol.*, 75:7537–7541.

Scholz, B., Guillou, L., Marano, A. V., Neuhauser, S., Sullivan, B. K., Karsten, U., Küpper, F. C. & Gleason, F. H. 2016. Zoosporic parasites infection marine diatoms – a black box that needs to be opened. *Fungal Ecol.*, 19:59–76.

Taoka, Y., Nagano, N., Okita, Y., Izumida, H., Sugimoto, S. & Hayashi, M. 2009. Extracellular enzymes produced by marine eukaryotes, thraustochytrids. *Biosci. Biotechnol. Biochem.*, 73:180–182.

Tsui, C. K. M., Marshall, W., Yokoyama, R., Honda, D., Lippmeier, J. C., Craven, K. D., Peterson, P. D. & Berbee, M. L. 2009. Labyrinthulomycetes phylogeny and its implications for the evolutionary loss of chloroplasts and gain of ectoplasmic gliding. *Mol. Phylogenet. Evol.*, 50:129–140.

Ueda, M., Nomura, Y., Doi, K., Nakajima, M. & Honda, D. 2015. Seasonal dynamics of culturable thraustochytrids (Labyrinthulomycetes, Stramenopiles) in estuarine and coastal waters. *Aquat. Microb. Ecol.*, 74:187–204.

White, T.J., Bruns, T., Lee, S. & Taylor, J. 1990. Amplification and direct sequencing of fungal ribosomal RNA genes for phylogenetics. *In:* Innis, M.A., Gelfand, D.H., Sninsky, J.J. & White, T.J. (ed.), PCR Protocols: A Guide to Methods and Applications. Academic Press, San Diego, CA. 38:315–322.

Yokoyama, R. & Honda, D. 2007. Taxonomic rearrangement of the genus *Schizochytrium* sensu lato based on morphology, chemotaxonomic characteristics, and 18S rRNA gene phylogeny (Thrasutochytriaceae, Labyrinthulomycetes): emendation for *Schizochytrium* and erection of *Aurantiochytrium* and *Oblongichytrium* gen. nov. *Mycoscience*, 48:199–211.

Yokoyama, R., Salleh, B. & Honda, D. 2007. Taxonomic rearrangement of the genus *Ulkenia* senu lato based on morphology, chemotaxonomical characteristics, and 18S rRNA gene phylogeny (Thraustochytriaceae, Labyrinthulomycetes): emendation for *Ulkenia* and erection of *Botryochytrium*, *Parietichytrium*, and *Sicyoidochytrium* gen. nov. *Mycoscience*, 48:329–341.

SUPPORTING INFORMATION

Additional supporting information may be found online in the Supporting Information section at the end of the article.

File S1. Alignment of Pan et al. (2017) used to generate Figure 5, expanded with *P. isakeiti*, used to create Figure 5.

Table S1. Table of NCBI accessions and associated taxa from Pan et al. (2017), expanded with *P. isakeiti*, used to create Figure 5.

Video S1. Zoospores using ectoplasmic threads to interact with surface of diatom frustule.